JBC ARTICLE

Author's Choice

Kinetic parameters of human aspartate/asparagine–β-hydroxylase suggest that it has a possible function in oxygen sensing

Received for publication, December 5, 2019, and in revised form, February 24, 2020 Published, Papers in Press, February 26, 2020, DOI 10.1074/jbc.RA119.012202

Lennart Brewitz, Anthony Tumber, and Christopher J. Schofield[1]

From the Chemistry Research Laboratory, University of Oxford, OX1 3TA Oxford, United Kingdom

Edited by Joseph M. Jez

Human aspartate/asparagine–β-hydroxylase (AspH) is a 2-oxoglutarate (2OG)–dependent oxygenase that catalyzes the post-translational hydroxylation of Asp and Asn residues in epidermal growth factor–like domains (EGFDs). Despite its biomedical significance, studies on AspH have long been limited by a lack of assays for its isolated form. Recent structural work has revealed that AspH accepts substrates with a noncanonical EGFD disulfide connectivity (*i.e.* the Cys 1–2, 3–4, 5–6 disulfide pattern). We developed stable cyclic thioether analogues of the noncanonical EGFD AspH substrates to avoid disulfide shuffling. We monitored their hydroxylation by solid-phase extraction coupled to MS. The extent of recombinant AspH-catalyzed cyclic peptide hydroxylation appears to reflect levels of EGFD hydroxylation observed *in vivo*, which vary considerably. We applied the assay to determine the kinetic parameters of human AspH with respect to 2OG, Fe(II), L-ascorbic acid, and substrate and found that these parameters are in the typical ranges for 2OG oxygenases. Of note, a relatively high K_m for O_2 suggested that O_2 availability may regulate AspH activity in a biologically relevant manner. We anticipate that the assay will enable the development of selective small-molecule inhibitors for AspH and other human 2OG oxygenases.

The human 2-oxoglutarate (2OG[2], α-ketoglutarate)–dependent aspartate/asparagine–β-hydroxylase (AspH, also called BAH or HAAH) catalyzes the hydroxylation of Asp and Asn residues in epidermal growth factor–like domains (EGFDs) in the endoplasmic reticulum. AspH employs Fe(II) as a co-factor, 2OG and O_2 as co-substrates producing succinate, and CO_2 as co-products (Fig. 1*a*) (1, 2). EGFDs of, *inter alia*, coagulation factors and extracellular matrix components such as notch and its ligands, fibrillins, and latent transforming growth factor-β–binding proteins bear the proposed consensus sequence for AspH-catalyzed Asp/Asn hydroxylation (3–5). However, the presence of a consensus sequence alone is not predictive of the extent to which EGFD Asp/Asn hydroxylation occurs *in vivo*. For example, Asp_{103} of human coagulation factor X (hFX) is reported to be hydroxylated quantitatively (6, 7), whereas Asp_{123} of hFVII is reported not to be hydroxylated (8). The factors that regulate the extent of EGFD Asp/Asn hydroxylation and the biochemical consequences of EGFD Asp/Asn hydroxylation are thus poorly understood.

Clinically observed mutations (*e.g.* as occur in the Traboulsi syndrome) in the AspH gene, likely resulting in the loss of oxygenase function, are associated with ophthalmologic defects (ectopia lentis) and facial dysmorphism (9–11). Animal model studies link AspH loss to developmental defects, potentially triggered by disrupted notch signaling (12). AspH levels are up-regulated in certain cancers, *e.g.* hepatocellular carcinoma and glioma (13, 14). One form of AspH is reported to be translocated to the tumor cell surface membrane, an observation correlating with enhanced cell motility and metastatic spread, and statistically reduced life expectancy of cancer patients (15–18). It is unknown how exactly AspH affects cell motility; the biochemical mechanisms, AspH interactions, and substrates underlying this phenotype are not identified, although an effect on notch signaling pathway is proposed (19–21).

More than 100 different human EGFD-containing proteins bear the apparent consensus sequence for Asp/Asn hydroxylation; some of these potential substrates are structurally complex and occasionally contain more than 30 EGFDs (4, 22). Simplified model systems are thus needed to inform on the molecular aspects of AspH biology. AspH activity assays could be applied to determine kinetic parameters of isolated AspH, analyze its substrate affinities, identify inhibitors, investigate how AspH activity is regulated by co-factor/co-substrate availability, investigate the factors determining the extent of *in vivo* EGFD Asp/Asn hydroxylation, and help unravel the mechanisms by which AspH controls cell motility. Such studies, however, have long been limited by the lack of robust assays for isolated AspH.

2OG oxygenases play a pivotal role in the hypoxic response by catalyzing the post-translational prolyl residue hydroxyl-

This work was supported by Wellcome Trust Grant 106244/Z/14/Z, Cancer Research UK Grant C8717/A18245, and Biotechnology and Biological Sciences Research Council Grant BB/J003018/1. This work was also supported by Deutsche Forschungsgemeinschaft Fellowship BR 5486/2-1 (to L. B.) The authors declare that they have no conflicts of interest with the contents of this article.

This article contains Figs. S1–S7.

[1] To whom correspondence should be addressed: Chemistry Research Laboratory, University of Oxford, 12 Mansfield Rd., OX1 3TA, Oxford, UK. Tel.: 44-1865-275625; E-mail: christopher.schofield@chem.ox.ac.uk.

[2] The abbreviations used are: 2OG, 2-oxoglutarate; AspH, aspartate/asparagine–β-hydroxylase; EGFD, epidermal growth factor–like domain; EGFL7, epidermal growth factor–like protein 7; FAS, ferrous ammonium sulfate; FIH, factor-inhibiting HIF; hFX, human coagulation factor X; HIF, hypoxia-inducible transcription factor; LAA, L-ascorbic acid; SPE, solid-phase extraction; PHD, HIF prolyl hydroxylase; TPR, tetratricopeptide repeat; KDM, lysine demethylase; SPPS, solid-phase peptide synthesis; Fmoc, *N*-(9-fluorenyl)methoxycarbonyl.

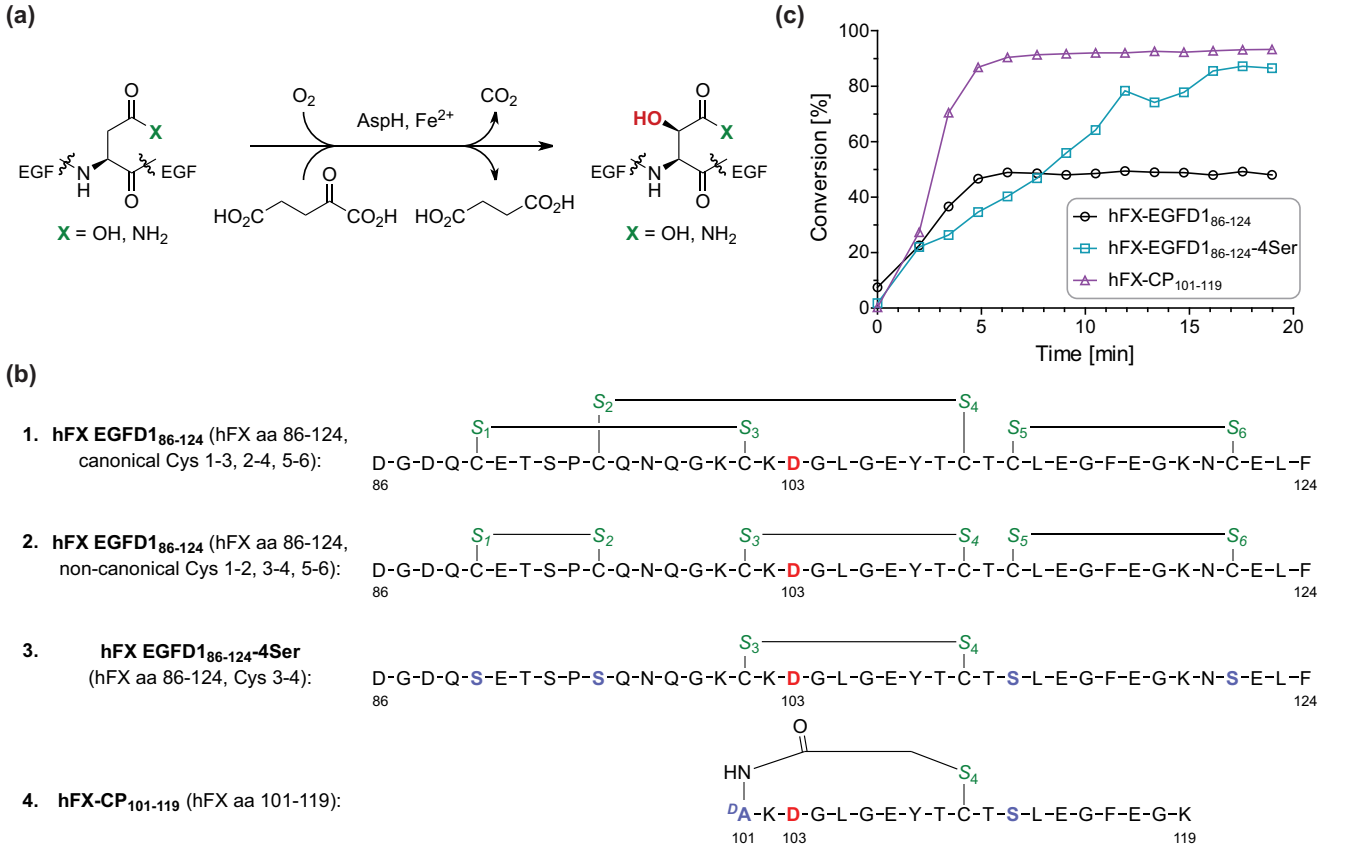

Figure 1. AspH-catalyzed hydroxylation. *a*, scheme for the diastereospecific AspH-catalyzed hydroxylation of Asp/Asn residues in EGFDs. *b*, structures of the canonical (*peptide 1*; Cys 1–3, 2–4, 5–6) and noncanonical (*peptide 2*; Cys 1–2, 3–4, 5–6) disulfide isomers of hFX–EGFD1$_{86-124}$, hFX–EGFD1$_{86-124}$-4Ser (*peptide 3*; Cys 3–4), and the cyclic thioether peptide hFX–CP$_{101-119}$ (*peptide 4*). The AspH-hydroxylation site (Asp103$_{hFX}$) is in *red*, cysteine sulfurs are in *green*; and substituted residues are in *light blue*. Numbering is according to the sequence of hFX. *c*, His$_6$–AspH$_{315-758}$ catalyzed Asp hydroxylation of hFX–EGFD1$_{86-124}$ (*black circles*, mixture of canonical and noncanonical disulfide isomers, *peptides 1* and *2* in Fig. 1*b*), hFX–EGFD1$_{86-124}$–4Ser (*peptide 3*, *turquoise squares*), and cyclic peptide hFX–CP$_{101-119}$ (*peptide 4*, *purple triangles*) in 50 mM HEPES buffer (pH 7.5, 20 °C). The reactions were performed as described under "Experimental procedures" using 0.1 μM His$_6$–AspH$_{315-758}$, 2.0 μM peptide substrate, 100 μM LAA, 10 μM FAS, and 10 μM 2OG. The measurement times were normalized to the first sample injection analyzed after the addition of the enzyme mixture to the substrate mixture (t = 0 min), by which time low levels of hydroxylation were manifest.

ation of the hypoxia-inducible transcription factors (HIFs) that work to ameliorate the effects of limited oxygen availability (hypoxia) (23, 24). 2OG-dependent HIF-α prolyl hydroxylase (PHD) activity is limited by oxygen availability. Prolyl hydroxylation signals for HIF-α degradation; hence the PHDs are proposed to act as hypoxia sensors (23–25). A second type of HIF-α hydroxylase, factor-inhibiting HIF (FIH), catalyzes HIF-α asparaginyl residue hydroxylation, a modification that serves to reduce the transcriptional activity of HIF (23–25). The HIF-α prolyl and asparaginyl residue hydroxylases contain the typical H*X*(D/E) . . . H triad of Fe(II)-binding ligands present in most 2OG oxygenases (25). The O_2-sensing ability of the PHDs is proposed to be reflected in their slow reaction with O_2, as manifested in high K_m and low k_{cat} values (26–29). By contrast, FIH is less susceptible to hypoxia (27, 30–32) and catalyzes the hydroxylation of other substrates than HIF, often from the ankyrin repeat domain–containing family of proteins (33, 34), where it can catalyze the hydroxylation of not only asparaginyl residues, but (like AspH) also of other residues including aspartyl residues (35).

Recently, we described biochemical and crystallographic analyses on AspH (36). The results showed that AspH has an unusual active site, bearing only two Fe(II) ligands (His$_{679}$ and His$_{725}$) rather than the typical H*X*(D/E)…H triad of Fe(II) ligands observed in most 2OG hydroxylases (36). The unusual active site geometry of AspH suggests that it may have the capacity to act as a sensor for Fe(II), 2OG, or O_2. The combined biochemical and crystallographic studies also revealed that AspH requires a noncanonical EGFD–disulfide connectivity (Cys 1–2, 3–4, 5–6), rather than the canonical EGFD–disulfide connectivity (Cys 1–3, 2–4, 5–6), for productive catalysis (36).

Here, we describe a label-free MS-based AspH activity assay using human His$_6$–AspH$_{315-758}$ and synthetic cyclic peptide AspH substrates. The new AspH assay was used to quantify substrate hydroxylation and applied to determine kinetic parameters of AspH for its Fe(II) co-factor, 2OG and O_2 co-substrates, and stable EGFD substrate analogues. The results suggest that AspH activity has the potential to be limited by O_2 availability, potentially in a hypoxia-sensing capacity.

Results

Development of an efficient AspH activity assay

In our initial report on the activity of AspH, we employed MALDI-MS end-point turnover assays (36). However, these assays required high-enzyme/substrate concentrations and

time-consuming sample matrix preparations. This, together with variations in sample ionization efficiencies, disfavors the use of the MALDI-MS assay for efficient high-throughput analyses. Pioneering assays using native AspH had monitored 2OG turnover; however, such assays can be misleading because 2OG oxidation can be decoupled from that of substrate; further, these assays likely involved EGFDs with mixed disulfide patterns (37–40). We therefore aimed to develop improved AspH assays employing defined and stable substrates to investigate the kinetic parameters and substrate selectivity of AspH.

Solid-phase extraction (SPE) coupled to MS was investigated as analytical method to monitor AspH activity. SPE-MS combines the advantages of high resolution MS as a direct label-free technique with the benefits of avoiding time-consuming sample preparation, thus minimizing measurement times. SPE-MS requires only small amounts of substrates/enzymes for analysis and has been successfully applied to monitoring the activity of 2OG oxygenases by measuring mass shifts, *i.e.* +16 Da for hydroxylation and −14 Da for demethylation (41–45). We aimed to combine SPE-MS with the use of stable substrate analogues in which the noncanonical Cys 3–4 EGFD disulfide bond was replaced with a stable thioether.

The initial synthetic substrates used in our study were derived from EGFD1 (amino acids 86–124) of human coagulation factor X (hFX), which is reported to be an AspH substrate in humans (6, 7). The peptides initially studied were hFX–$EGFD1_{86-124}$ (which is a mixture of canonical and noncanonical disulfide isomers; Fig. 1*b*, *peptides 1/2*), hFX–$EGFD1_{86-124}$-4Ser (which has the noncanonical Cys 3–4 EGFD disulfide with the other four cysteine residues substituted for serine residues; Fig. 1*b*, *peptide 3*), and the thioether-linked cyclic peptide hFX–$CP_{101-119}$ (Fig. 1*b*, *peptide 4*). The three substrates all had an aspartyl residue at the hydroxylation site.

The cyclic thioether of hFX–$CP_{101-119}$ (Fig. 1*b*, *peptide 4*) was prepared via reaction of the $Cys110_{hFX}$ thiol with an N-terminal chloroacetyl group and mimics the noncanonical Cys 3–4 EGFD substrate disulfide, while being more stable than a disulfide (36). The three peptides 2, 3, and 4 (Fig. 1*b*) bind to AspH in a catalytically productive manner as evidenced by crystallographic analysis (Fig. S1) (36). The peptides and their hydroxylation products were analyzed by SPE-MS monitoring substrate depletion and product formation (+16 Da mass shift). Initially, the assay conditions were optimized (Fig. S2). The highest AspH activity was observed in 50 mM HEPES buffer (pH 7.5) without additional salts in the presence of 2OG, ferrous ammonium sulfate (FAS), and L-ascorbic acid (LAA, which enhances the activity of many isolated 2OG oxygenases) (Fig. 1*c*) (46–48). Compared with our previously reported MALDI-MS assay conditions (36), the AspH concentration was reduced 100-fold to 0.1 μM in the SPE-MS based assay, significantly reducing the enzyme required, thus potentially more accurately reflecting physiological conditions.

Among the three synthetic AspH substrates investigated, the stable thioether-linked cyclic peptide hFX–$CP_{101-119}$ (Fig. 1*b*, *peptide 4*), which mimics the noncanonical Cys 3–4 hFX EGFD1 disulfide, was most efficiently hydroxylated (Fig. 1*c*). The hydroxylation of hFX–$CP_{101-119}$ and hFX–$EGFD1_{86-124}$ proceeded initially at a comparable rate, implying that the cyclic peptide hFX–$CP_{101-119}$ is a good model system to reflect the hydroxylation of the full-length hFX–$EGFD1_{86-124}$ peptide.

The hFX–$EGFD1_{86-124}$ peptide exists as a mixture of the canonical (Cys 1–3, 2–4, 5–6, the major form; Fig. 1*b*, *peptide 1*) and noncanonical (Cys 1–2, 3–4, 5–6, the minor form; Fig. 1*b*, *peptide 2*) disulfide isomers in solution, of which only the noncanonical isomer is a substrate for AspH (36). Consistent with this, hFX–$EGFD1_{86-124}$ hydroxylation was observed to slow after 5 min, reflecting complete consumption of the active noncanonical disulfide isomer (~45% conversion; Fig. 1*c*). Although the hydroxylation of hFX–$EGFD1_{86-124}$ can be driven to completion, *i.e.* by adding redox-active tripeptide GSH to the assay enabling disulfide isomerization (36), the presence of such reactive components in the assay is undesirable because they may limit applications such as the profiling of small-molecule AspH inhibitors (GSH might react with redox-active small molecules). Furthermore, disulfide isomerization is relatively slow at 20 °C, complicating kinetic analysis when using the hFX–$EGFD1_{86-124}$ disulfide mixture (Fig. 1*b*, *peptides 1* and *2*) as an AspH substrate.

In an attempt to circumvent the problems caused by hFX–$EGFD1_{86-124}$ disulfide isomerism, AspH-catalyzed hydroxylation of an hFX–$EGFD1_{86-124}$-derivative with only one disulfide, *i.e.* hFX–$EGFD1_{86-124}$-4Ser (Fig. 1*b*, *peptide 3*), was investigated (Fig. 1*c*). However, hydroxylation of hFX–$EGFD1_{86-124}$-4Ser was relatively slow compared with the other substrates, which might reflect a more disordered secondary structure in solution caused by the substitution of four cysteines/two cystine links by serine residues. We therefore pursued further studies using the synthetic thioether-linked cyclic peptide hFX–$CP_{101-119}$ AspH substrate (Fig. 1*b*, *peptide 4*). This has the additional benefit that its synthesis is straightforward and cost-effective.

Validation of the thioether-linked cyclic peptide as an AspH substrate

The thioether-linked cyclic peptide hFX–$CP_{101-119}$ (Fig. 1*b*, *peptide 4*) was then further validated as a tool to monitor AspH activity. Only a single AspH-catalyzed oxidation event (+16-Da mass shift) was observed under the assay conditions, *i.e.* no overoxidized cyclic peptides (+32 or +48 Da mass shifts) were observed by SPE-MS (Fig. S3). No oxidation of hFX–$CP_{101-119}$ was observed under the assay conditions in the absence of His_6–$AspH_{315-758}$. Taken together, these experiments show that oxidation of the thioether sulfur atom does not account for the observed mass difference of +16 Da (Fig. S3), in agreement with previous NMR experiments indicating that AspH oxidized Asp_{103hFX} of a thioether-linked cyclic peptide with a shorter sequence (hFX–$CP_{101-110}$) (36).

To investigate whether SPE-MS analysis of hFX–$CP_{101-119}$ can be used to quantify AspH activity, the ion counts of product (hydroxylated) and substrate (nonhydroxylated) cyclic peptides were analyzed as a function of time (Fig. S3); the sum of the ion counts was constant throughout the time course, confirming that SPE-MS is a useful technique to quantify AspH activity using the cyclic peptide hFX–$CP_{101-119}$ as substrate.

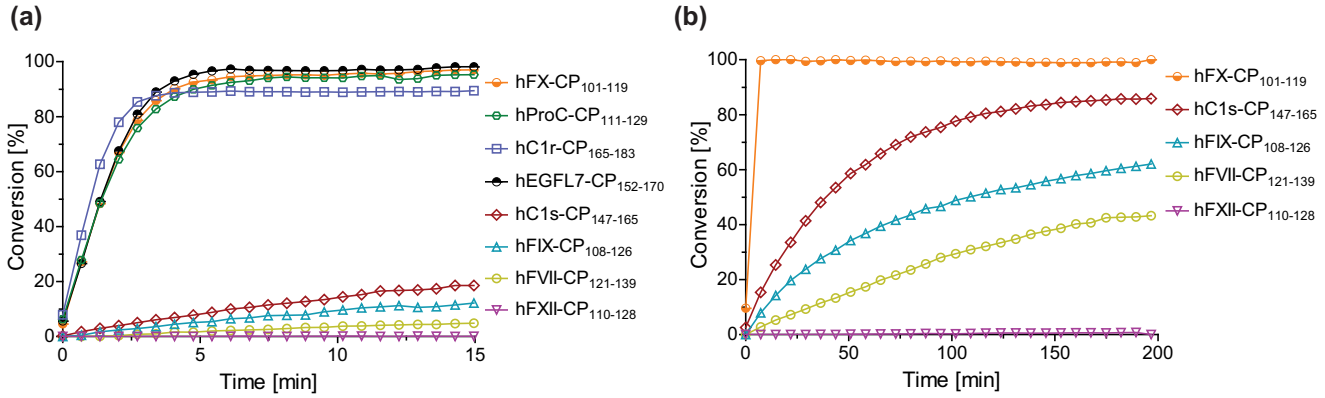

Figure 2. Time course of the AspH-catalyzed hydroxylation of different thioether-linked cyclic peptides corresponding to reported AspH substrates and controls. *a*, His_6–$AspH_{315–758}$ hydroxylates the cyclic peptides hProC–$CP_{111–129}$ (*green*), hC1r–$CP_{165–183}$ (*lavender*), and hEGFL7–$CP_{152–170}$ (*black*) efficiently with complete hydroxylation being observed in less than 15 min in a manner similar to hFX–$CP_{101–119}$ (*orange*). Hydroxylation of hC1s–$CP_{147–165}$ (*red*), hFVII–$CP_{121–139}$ (*yellow*), and hFIX–$CP_{108–126}$ (*cyan*) is considerably slower. No hydroxylation of hFXII–$CP_{110–128}$ (*pink*) was observed. *b*, His_6–$AspH_{315–758}$ catalyzes the hydroxylation of hFX–$CP_{101–119}$ (*orange*) apparently instantaneously, whereas hFXII–$CP_{110–128}$ (*pink*) is not hydroxylated even when incubated with AspH for 200 min. Hydroxylation of hC1s–$CP_{147–165}$ (*red*), hFVII–$CP_{121–139}$ (*yellow*), and hFIX–$CP_{108–126}$ (*cyan*) proceeds relatively slowly over 200 min. The reactions were performed as described under "Experimental procedures" using 0.1 μM His_6–$AspH_{315–758}$, 2.0 μM peptide, 100 μM LAA, 10 μM FAS, and 10 μM 2OG in 50 mM HEPES buffer (pH 7.5, 20 °C). The measurement times were normalized to the first sample injection analyzed after the addition of the enzyme mixture to the substrate mixture ($t = 0$ min), by which time low levels of hydroxylation were manifest. Peptide structures are shown in Fig. S4.

To investigate the extent to which hydroxylation of thioether-linked cyclic peptides reflect literature-reported EGFD Asp/Asn-hydroxylation levels in humans, thioether-linked cyclic peptides were synthesized based on the amino acid sequences of reported human AspH substrate proteins other than hFX: human coagulation factor VII (hFVII–$CP_{121–139}$) (8), human coagulation factor IX (hFIX–$CP_{108–126}$) (7), human protein C (hProC–$CP_{111–129}$) (49, 50), human complement C1r subcomponent (hC1r–$CP_{165–183}$) (51, 52), and human complement C1s subcomponent (hC1s–$CP_{147–165}$) (51, 53). These potential substrates include examples with both an aspartyl and an asparaginyl residue at the hydroxylation site. As a potential negative control, a cyclic peptide was synthesized based on the sequence of human coagulation factor XII (hFXII–$CP_{110–128}$), which does not bear the AspH consensus sequence (50). A cyclic peptide based on the sequence of human epidermal growth factor–like protein 7 (hEGFL7–$CP_{152–170}$), which as yet has not been associated with AspH biology, but which bears the predicted AspH substrate consensus sequence, was also synthesized. The relative sequence length (19 amino acids) and secondary structure (position of the thioether linkage) of the cyclic peptides are similar to hFX–$CP_{101–119}$ (Fig. 1*b*, *peptide 4*) as shown in Figs. S1 and S4. The cyclic peptides were incubated with His_6–$AspH_{315–758}$ under the optimized assay conditions; the extent of their Asp/Asn hydroxylation was monitored using SPE-MS (Fig. 2, Table 1, and Fig. S4).

The results of screening the AspH-catalyzed hydroxylation of the different thioether-linked cyclic peptides are summarized in Table 1, which compares the results with literature-reported *in vivo* hydroxylation levels of the human AspH substrate proteins. The results support previous studies showing that AspH can catalyze efficiently hydroxylation of both Asp and Asn residues. Importantly, the relative extent of cyclic peptide hydroxylation correlates well with the relative levels of both EGFD Asp and Asn hydroxylation observed *in vivo*. For example, hFX–$CP_{101–119}$ is more efficiently hydroxylated by AspH under the assay conditions than hFIX–$CP_{108–126}$, which itself is a better substrate than hFVII–$CP_{121–139}$. The cyclic peptides hProC–$CP_{111–129}$, hC1r–$CP_{165–183}$, and hEGFL7–$CP_{152–170}$ are as efficiently hydroxylated as hFX–$CP_{101–119}$ upon short exposure times to AspH (<15 min), in apparent agreement with the reported *in vivo* EGFD hydroxylation levels for human protein C (49, 50) and C1r (51, 52). The hydroxylation of hFIX–$CP_{108–126}$, hFVII–$CP_{121–139}$, and hC1s–$CP_{147–165}$ was incomplete even after a prolonged exposure time of 200 min (Table 1), again reflecting the reported *in vivo* human EGFD hydroxylation levels (7, 8, 51, 53).

For all the tested cyclic peptides, only one oxidation event (+16-Da mass shift) was observed, with the exception of hFXII–$CP_{110–128}$, which was not a substrate. Together with the divergent hydroxylation levels, this observation further confirms the proposal that AspH selectively catalyzes the anticipated β-oxidation of Asp/Asn residues. No hydroxylation of the thioether-linked cyclic peptide hFXII–$CP_{110–128}$, which contains a methionine residue in its sequence, was observed supporting the proposal that the consensus sequence C*X*(D/N)*XXXX*(F/Y)*X*C for AspH-catalyzed Asp/Asn hydroxylation in EGFDs is valid. The essential consensus sequence hydrophobic Phe/Tyr residue, which interacts with a hydrophobic pocket located in the AspH tetratricopeptide repeat (TPR) domain (Fig. S1) (36), is substituted by a proline in hFXII–$CP_{110–128}$, explaining its lack of activity. Having confirmed that thioether-linked cyclic peptides are useful model systems that apparently reflect *in vivo* AspH-catalyzed human EGFD oxidation, we next focused on determining kinetic parameters for AspH.

AspH kinetic parameters

The kinetic characterization of His_6–$AspH_{315–758}$ with respect to its co-factor and (co-)substrates was then performed under the optimized SPE-MS assay conditions using the stable thioether-linked cyclic peptide hFX–$CP_{101–119}$ (Fig. 1*b*, *peptide 4*) as a substrate. To our knowledge, kinetic data of AspH have so far only been reported using the partially purified native bovine-derived AspH and peptides based on the sequence of

Table 1
AspH-catalyzed hydroxylation of thioether-linked cyclic peptides based on the EGFD sequences of human proteins

	Peptide substrate[a]	Hydroxylation		Reported *in vivo* EGFD Asp/Asn-hydroxylation levels in humans	
		t = 15 min	t = 200 min	Values	Sources
		%		%	
1	hFX–$CP_{101–119}$ (Fig. 1*b*, *peptide 4*)	>95	>95	89–100	Refs. 6, 7, and 63
2	hProC–$CP_{111–129}$	>95	ND[b]	89–100	Refs. 49 and 50
3	hEGFL7–$CP_{152–170}$	>95	ND		[c]
4	hC1r–$CP_{165–183}$	~90	ND[d]	90	Refs. 51 and 52
5	hC1s–$CP_{147–165}$	~20	~85	~50	Refs. 51 and 53
6	hFIX–$CP_{108–126}$	~12	~60	26	Ref. 7
7	hFVII–$CP_{121–139}$	~5	~40	0	Ref. 8
8	hFXII–$CP_{110–128}$	<1	<1	0	Ref. 50

[a] The sequences and structures of the cyclic peptides are shown in Fig. S4.
[b] ND, not determined.
[c] Note that human EGFL7 is not a reported substrate of AspH.
[d] $Asn167_{hC1r}$ hydroxylation did not appear to increase beyond ~90% substrate conversion.

hFX and hFIX (with undefined disulfide connectivity) as substrates, with monitoring by 2OG turnover (38–40).

Initially, we determined the concentration of active His_6–$AspH_{315–758}$ by performing an active site titration using the tight binding small-molecule AspH inhibitor pyridine–2,4-dicarboxylic acid (38, 54). Based on the SPE-MS experiments, the total concentration of active His_6–$AspH_{315–758}$ was calculated to be 90.8 ± 13.7 nM with an original estimated AspH assay concentration of 100 nM (Fig. 3). Based on the calculated concentration of active enzyme, both turnover numbers (catalytic constants, k_{cat}) and specificity constants (k_{cat}/K_m) were then determined (see below). Turnover numbers using hFX–$CP_{101–119}$ as an AspH substrate were, within the experimental error, constant throughout all kinetic experiments (Table 2), indicating good data quality and accuracy of the SPE-MS AspH activity assay.

The apparent Michaelis constant (K_m^{app}) for the AspH co-factor Fe(II) was determined to be ~4.8 μM using FAS as the iron source (Fig. 4*a* and Table 2). The K_m^{app} of AspH for Fe(II) is in the range of those reported for bovine AspH (3 μM) (38) and other human asparaginyl and prolyl residue hydroxylases (30). This observation suggests that the unusual Fe(II)-binding site of AspH, which is composed of only two ligands (His_{679} and His_{725}) rather than the typical three, is not reflected in an unusual K_m^{app} value.

LAA is commonly added to assay buffers to enhance the activity of isolated 2OG oxygenases (*e.g.* for the procollagen and HIF-α prolyl hydroxylases) (46–48). In some cases LAA might act as a co-substrate, effectively replacing 2OG (*e.g.* certain TET (ten-eleven translocation) type oxygenases (55) and the plant enzyme ACCO (1-aminocyclopropane-1-carboxylate oxidase) (56, 57)). AspH activity was sensitive toward subtle changes in the redox environment, possibly because of redox active species formation in iron-containing buffers (58). LAA is a useful component of the AspH assay buffer because it improves assay robustness, possibly by scavenging reactive oxidizing species and/or maintaining the Fe(II) form of iron. The use of physiologically relevant concentrations of LAA (59) also increased assay accuracy when determining the K_m^{app} for Fe(II) (Fig. 4*b*). In the absence of LAA, the K_m^{app} for Fe(II) is approximately four times higher than in its presence (~4.8 and ~1.4 μM, respectively). However, when investigating the kinetic effect of LAA on AspH catalysis at saturating 2OG co-substrate and Fe(II) concentrations, LAA did not affect k_{cat} values within experimental error (Fig. 4*c* and Table 2).

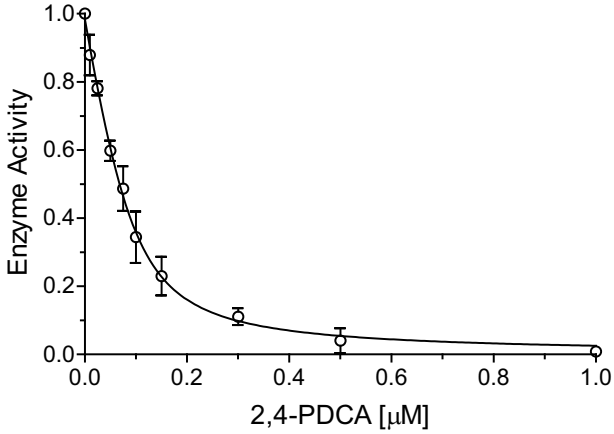

Figure 3. Active site titration of AspH using pyridine-2,4-dicarboxylic acid (2,4-PDCA) as a tight binding inhibitor. The data are shown as the mean averages of three independent runs (n = 3; means ± S.D.). AspH activity was normalized against a DMSO control. Initial peptide hydroxylation rates are shown in Fig. S5.

Determining the K_m^{app} for the AspH co-substrate 2OG by monitoring substrate hydroxylation is feasible as AspH-catalyzed 2OG turnover only proceeds at a low rate in the absence of substrate (36). The 2OG K_m^{app} of AspH was determined to be ~0.6 μM (Fig. 4*d* and Table 2). This is in the range of 2OG K_m^{app} values reported for bovine AspH (~5 μM) (38) and most other human 2OG oxygenases, including the PHDs and FIH (1–25 μM) (60). The 2OG K_m^{app} of AspH is significantly smaller than reported cellular 2OG levels in healthy cells (61). It is also considerably less than the 2OG K_m^{app} value of γ-butyrobetaine hydroxylase, the activity of which has the potential to be limited by *in vivo* 2OG availability (62).

The K_m of AspH for the thioether-linked cyclic peptide hFX–$CP_{101–119}$ (Fig. 1*b*, *peptide 4*) was determined to be ~1.2 μM (Fig. 5*a* and Table 2). This is lower than that reported for bovine AspH for an hFX EGFD1-derived peptide substrate (~30 μM), which is likely a mixture of disulfide isomers (38). By contrast with previous observations using bovine AspH and an hFX EGFD1-derived peptide substrate (38), neither hFX–$CP_{101–119}$ nor its hydroxylated product inhibited AspH activity at higher concentrations (up to 16 μM hFX–$CP_{101–119}$). However, the values are difficult to compare because human hFX EGFD1 is not the natural substrate of bovine AspH. Further, variations in

Table 2

Steady-state kinetic parameters for AspH

Maximum velocities (v_{max}), Michaelis constants (K_m), turnover numbers (k_{cat}), and specificity constant (k_{cat}/K_m) of His_6–$AspH_{315–758}$ for its Fe(II) cofactor, 2OG and O_2 co-substrates, LAA, and substrates. The values are the mean averages of three independent runs ($n = 3$; means ± S.D.).

		v_{max}	K_m	k_{cat}	k_{cat}/K_m
		$\mu M\ s^{-1}$	μM	s^{-1}	$\mu M^{-1} \cdot s^{-1}$
1	Fe(II)[a,b]	$16.8 \times 10^{-3} \pm 0.4 \times 10^{-3}$	4.76 ± 0.48	0.19 ± 0.03	0.04 ± 0.01
2	Fe(II) [a,c]	$17.1 \times 10^{-3} \pm 0.5 \times 10^{-3}$	1.42 ± 0.16	0.19 ± 0.03	0.13 ± 0.03
3	LAA[a]	$14.9 \times 10^{-3} \pm 2.1 \times 10^{-3}$		0.16 ± 0.03	
4	2OG[a]	$16.8 \times 10^{-3} \pm 0.5 \times 10^{-3}$	0.60 ± 0.09	0.19 ± 0.03	0.32 ± 0.07
5	hFX–$CP_{101–119}$	$17.8 \times 10^{-3} \pm 1.3 \times 10^{-3}$	1.19 ± 0.26	0.20 ± 0.03	0.17 ± 0.05
6	hProC–$CP_{111–129}$	$15.6 \times 10^{-3} \pm 0.6 \times 10^{-3}$	1.71 ± 0.21	0.17 ± 0.03	0.10 ± 0.02
7	hEGFL7–$CP_{152–170}$	$22.8 \times 10^{-3} \pm 4.3 \times 10^{-3}$	2.04 ± 0.65	0.25 ± 0.06	0.12 ± 0.05
8	hC1r–$CP_{165–183}$	$41.0 \times 10^{-3} \pm 7.0 \times 10^{-3}$	3.00 ± 0.79	0.45 ± 0.10	0.15 ± 0.05
9	hC1s–$CP_{147–165}$	$10.9 \times 10^{-3} \pm 0.6 \times 10^{-3}$	36.5 ± 5.1	0.12 ± 0.02	$3.3 \times 10^{-3} \pm 0.7 \times 10^{-3}$
10	O_2[a,d]	$20.7 \times 10^{-3} \pm 1.8 \times 10^{-3}$	426 ± 73	0.23 ± 0.04	$5.4 \times 10^{-4} \pm 1.3 \times 10^{-4}$

[a] The v_{max}^{app} and K_m^{app} values were determined monitoring the hydroxylation of hFX–$CP_{101–119}$ (Fig. 1*b*, *peptide 4*).
[b] In the absence of LAA.
[c] In the presence of LAA.
[d] Mean averages of four independent runs ($n = 4$; means ± S.D.).

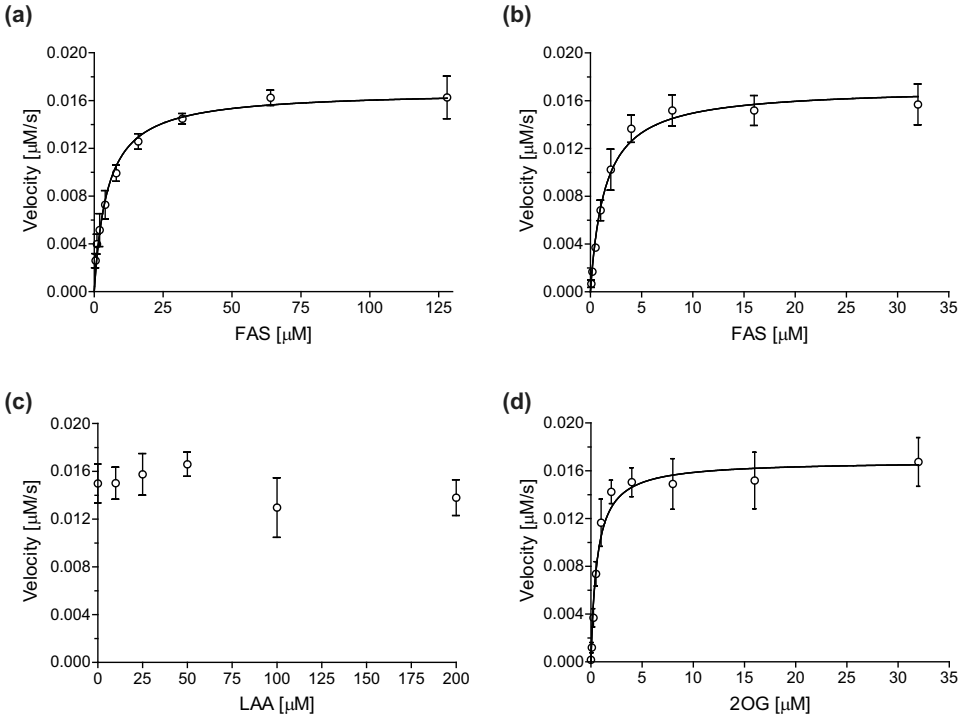

Figure 4. Determination of steady-state kinetic parameters for AspH from initial hydroxylation rates of the thioether-linked cyclic peptide hFX–$CP_{101–119}$ (Fig. 1*b*, *peptide 4*). *a*, K_m^{app} of AspH for FAS in the absence of LAA. *b*, K_m^{app} of AspH for FAS in the presence of LAA. *c*, effect of LAA on AspH activity. *d*, K_m^{app} of AspH for 2OG. The data are shown as the mean averages of three independent runs ($n = 3$; means ± S.D.). The results are summarized in Table 2. Initial peptide hydroxylation rates are shown in Fig. S6.

enzyme purity (partial for the bovine AspH *versus* high purified recombinant human AspH) and assay techniques (scintillation counting monitoring 2OG turnover (38) *versus* our SPE-MS) may result in different absolute values.

The combined results presented here and previously (36) reveal EGFD folding and/or disulfide isomerization influences AspH catalysis. The thioether-linked cyclic peptide hFX–$CP_{101–119}$ (Fig. 1*b*, *peptide 4*) comprises the active site binding Cys 3–4 disulfide–containing element of EGFD AspH substrates, as well as the TPR domain–binding residues, as based on crystallographic analyses of AspH substrate complexes (Fig. S1), including with the noncanonical hFX EGFD1 disulfide isomer (Cys 1–2, 3–4, 5–6) (36). The cyclic structure of hFX–$CP_{101–119}$ lacks the capability for disulfide isomerization that may complicate AspH hydroxylation kinetics. The cyclic thioether strategy thus seems to be a useful method for investigating the observed divergent hydroxylation levels of different AspH substrates that are observed in humans (Table 1).

Determining the K_m and k_{cat} values for the different thioether-linked cyclic peptides enables rationalization of their observed relative hydroxylation efficiencies (Fig. 2). For example, both K_m (~1.7 μM) and k_{cat} (~0.17 s^{-1}) for hProC–$CP_{111–129}$ are similar to those of hFX–$CP_{101–119}$ (Fig. 5, *a* and *b*, and Table 2), suggesting similar hydroxylation efficiencies. These kinetic parameters are consistent with the similar EGFD hydroxylation levels of hFX and ProC that are observed in humans (Table 2) (6, 7, 49, 50, 63). In the case of the hC1r–$CP_{165–183}$ and hEGFL7–$CP_{152–170}$, substrate inhibition was observed at higher substrate concentrations (>4 μM; Fig. 5, *c* and *e*). This observation is in agreement with a previous report on substrate inhibition dur-

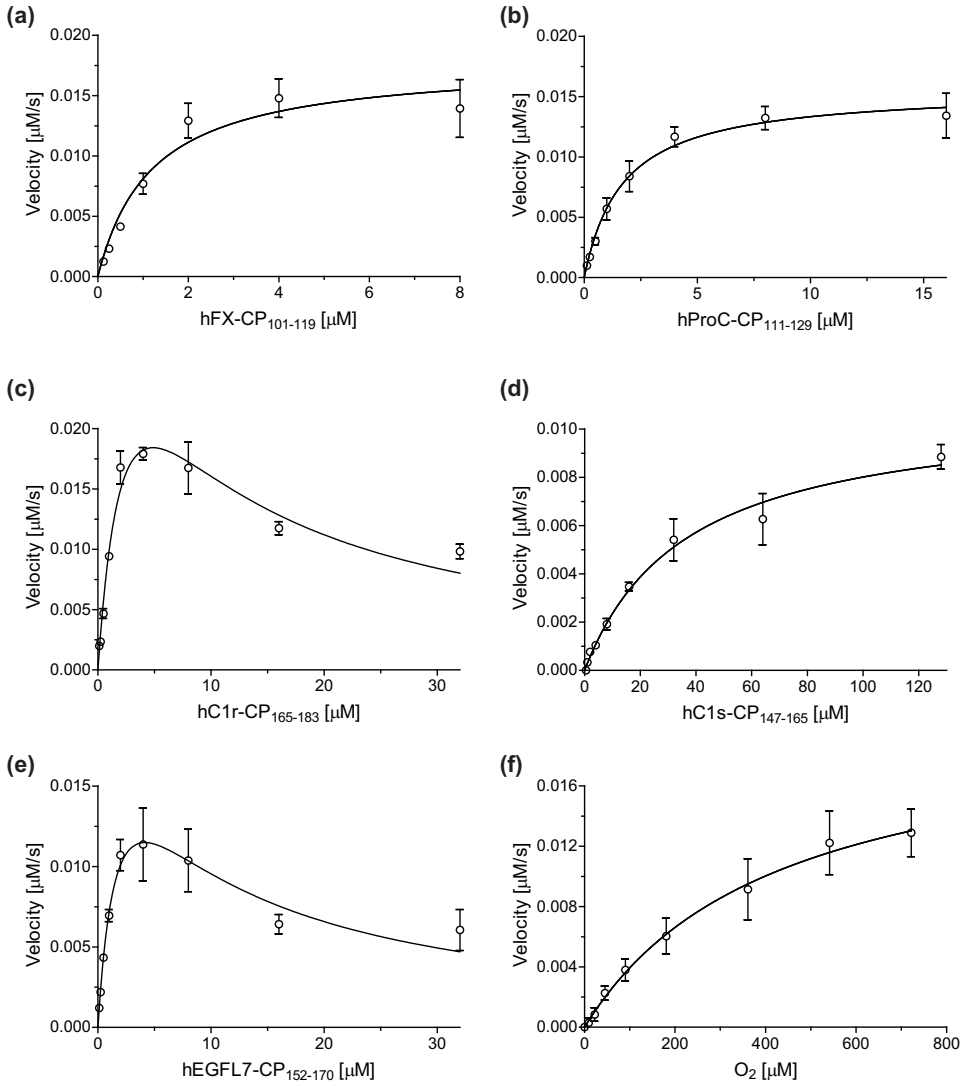

Figure 5. Determination of steady-state kinetic parameters for AspH from initial hydroxylation rates of thioether-linked cyclic peptides. *a*, K_m of AspH for the cyclic peptide hFX–$CP_{101–119}$ (Fig. 1*b*, *peptide 4*). *b*, K_m of AspH for the cyclic peptide hProC–$CP_{111–129}$. *c*, K_m of AspH for the cyclic peptide hC1r–$CP_{165–183}$. *d*, K_m of AspH for the cyclic peptide hC1s–$CP_{147–165}$. *e*, K_m of AspH for the cyclic peptide hEGFL7–$CP_{152–170}$. *f*, K_m^{app} of AspH for O_2 monitoring the hydroxylation of thioether-linked cyclic peptide hFX–$CP_{101–119}$ (Fig. 1*b*, *peptide 4*). The data are shown as the mean averages of three independent runs ($n = 3$; means ± S.D.) and for *f* as the mean averages of four independent runs ($n = 4$; means ± S.D.). The results are summarized in Table 2. Initial peptide hydroxylation rates are shown in Figs. S6 and S7.

ing the hydroxylation of hFX using bovine AspH (38). Nonetheless, the kinetic parameters suggest that similar *in vivo* EGFD Asp/Asn-hydroxylation levels might be anticipated for human EGFL7 and C1r. Human EGFD Asp/Asn-hydroxylation levels have been reported for C1r to be ~90% (Table 1) (51, 52). Our kinetic parameters for hC1s–$CP_{147–165}$ indicate that AspH has a considerably lower affinity for C1s (K_m = ~36.5 μM) and hydroxylates it slightly less efficiently (k_{cat} = ~0.12 s^{-1}) than hFX, ProC, and C1r, in accord with the reported *in vivo* results (51, 53). Kinetic parameters for the cyclic peptides hFVII–$CP_{121–139}$ and hFIX–$CP_{108–126}$ could not be determined because of their inefficient hydroxylation.

The experimental setup was modified to determine the K_m^{app} for O_2: the AspH K_m^{app} for O_2 was ~426 μM under stationary condition using different partial pressures of O_2 (Fig. 5*f* and Table 2). At higher partial pressures of O_2, the standard deviation among independent quadruplicates increased slightly because of efficient peptide hydroxylation requiring short reaction times; however, maximum velocities (v_{max}^{app}) were still similar within experimental error, indicating good data quality and reproducibility (Fig. S7). The AspH K_m^{app} for O_2 is high compared with the values reported for most other human 2OG oxygenases and JmjC lysine demethylases (KDMs): only the $K_m^{app}(O_2)$ values of the HIF-α prolyl hydroxylases (PHD1–3), which range between 230 and 1746 μM (26–28), are considerably higher than the one of AspH. The $K_m^{app}(O_2)$ values for FIH (90 to 237 μM) (27, 30, 31), human phytanoyl-CoA hydroxylase (93 ± 43 μM) (27), the collagen prolyl 4-hydroxylases (40 μM) (26), KDM4A (57 ± 10 μM) (64), KDM4C (158 ± 13 μM) (64), KDM4E (197 ± 16 μM) (64), and KDM6A (180 ± 40 μM) (65) are all lower than for AspH and the PHDs. Under the identical experimental setup, the $K_m^{app}(O_2)$ values of FIH (~110 μM) (32) and KDM4A (~173 μM) (66) were at least two times lower than the AspH K_m^{app} (Table 3), whereas PHD2 showed an apparently

Table 3
Reported Michaelis constants (K_m^{app}) and turnover numbers (k_{cat}) of 2OG oxygenases for O_2 using the same experimental setup as employed in our work

	2OG oxygenase	Peptide substrate	K_m^{app} for O_2	k_{cat}
			μM	s^{-1}
1	AspH	hFX–$CP_{101-119}$	426 ± 73	0.23 ± 0.04
2	FIH (32)	HIF-1α CAD_{35mer}[a]	110 ± 30	0.56 ± 0.04
3	PHD2 (32)	HIF-1α CODD[b]	460 ± 30	0.06 ± 0.01
4	PHD2 (32)	HIF-1α NODD[c]	>450	0.028 ± 0.001
5	KDM4A (66)	$H3_{1-15}$K9me3	173 ± 23	ND[d]

[a] C-terminal transactivation domain (CAD, HIF-1α amino acids 789–822).
[b] C-terminal oxygen-dependent degradation domain (CODD, HIF-1α amino acids 556–574).
[c] N-terminal oxygen-dependent degradation domain (NODD, HIF-1α amino acids 395–413).
[d] ND, not determined.

even weaker affinity for dioxygen (>450 μM) (32). Notably, although the $K_m^{app}(O_2)$ value for AspH appears relatively high, turnover number (k_{cat}) comparison indicates a more efficient substrate hydroxylation for AspH compared with PHD2 under substrate saturating conditions (Table 3).

DICUSSION

Several lines of evidence suggest that AspH is a physiologically important 2OG oxygenase. These include its conserved nature in animals and likely presence in earlier organisms (36), links between mutations in the AspH encoding genes to inherited diseases (9–11), links of AspH to cancer (13, 15–17), mouse model studies (12), and analytical studies revealing extensive hydroxylation of (likely) AspH-catalyzed hydroxylation of EGFDs (3, 5–7, 67). Notably, the latter manifest to very different levels, suggesting the poised nature of AspH catalyzed hydroxylation (3, 6–8), a property that may be useful in a sensing or regulatory capacity. Work on the molecular roles of AspH has, however, been limited by a lack of robust assays for it in isolated form.

We developed a real-time AspH activity assay using SPE-MS and our recently reported soluble His_6–$AspH_{315-758}$ construct (36). The results with both disulfide fragments of hFX (Fig. 1*b*, *peptides 1/2* and *3*) and a thioether-linked cyclic peptide (hFX–$CP_{101-119}$; Fig. 1*b*, *peptide 4*) support the proposal that AspH accepts EGFDs with the noncanonical (Cys 1–2, 3–4, 5–6) rather than the canonical (Cys 1–3, 2–4, 5–6) disulfide pattern. The thioether-linked cyclic peptide hFX–$CP_{101-119}$ was identified as useful substrate to monitor AspH activity because its synthesis is straightforward, it is conformationally stable, and it is efficiently hydroxylated. Consistent with the prior literature (3), both Asp and Asn residues can be hydroxylated by AspH in an EGFD sequence context–dependent manner. Hydroxylation occurs at a single Asp/Asn residue, and hydroxylation can be readily quantified by SPE-MS analysis (Fig. 1 and Fig. S2).

The results support the proposal that SPE-MS is an excellent analytical technique for 2OG oxygenase assays: its high sensitivity requires only low enzyme and substrate concentrations for analysis, sample preparation is efficient because label-free MS-analysis is performed *in situ*, resulting in short overall measurement times (Fig. 1), and it does not suffer from the false positive/negative drawbacks of coupling 2OG oxygenase catalysis to other enzymes, using antibody-based detection or measuring co-substrate/co-product formation (68).

The SPE-MS assay was applied to determine kinetic parameters of human AspH for its substrates, Fe(II), and co-substrates (Figs. 4 and 5 and Table 2). There is the possibility that the kinetic parameters of AspH will vary depending on the substrate (sequence) identity, the form of the substrate, and/or the form of AspH. Indeed, there is precedent for each of these variables affecting 2OG oxygenase catalysis (69). For example, FIH, which like AspH accepts many substrates (and catalyzes the hydroxylation of both asparaginyl and aspartyl residues), manifests varying efficiencies with respect to its substrates both in isolated form and in cells (35, 70). The conformations of FIH substrates can also affect the efficiency of their hydroxylation (34). This conformational effect is even more strikingly evidenced in the preference of AspH for a noncanonical EGFD substrate disulfide pattern (Cys 1–2, 3–4, 5–6) rather than the canonical pattern (Cys 1–3, 2–4, 5–6), as observed in multiple crystal structures (36). Like AspH, where its TPR domain is important in catalysis (36), the activities of at least some JmjC KDMs are affected by noncatalytic domains, as exemplified by the cases of KDM7A/B (71). Thus, care should be taken in assuming that parameters determined for isolated truncated enzyme are necessarily relevant in a physiological context. Despite these caveats, the results of the initial kinetic characterization reported here on AspH are of interest, especially with respect to a potential role for AspH in redox regulation, including the hypoxic response.

The K_m^{app} value of AspH for O_2 is notably high compared with most other 2OG oxygenases for which data are reported (Table 3), with only the PHDs being more sensitive toward changes in O_2 availability under substrate saturating conditions (26–28). Further, detailed kinetic studies on AspH are of interest including with respect to determining the molecular basis for its high K_m^{app} for O_2, which in the case of PHD2 (the most conserved and likely most important hypoxia sensor of the three human PHDs (72)) is proposed, on the basis of biophysical and kinetic studies, to result from slow binding of O_2 to the active site Fe(II), potentially in part, because of a requirement to displace a tightly ligated water (29, 73). It should also be noted that the $k_{cat}(O_2)$ value for AspH is substantially higher than that for PHD2 (Table 3). Nonetheless, coupled with the observation of varied levels of EGFD hydroxylation (3, 6–8), our observation of an unusually high K_m^{app} of AspH with otherwise more typical kinetic parameters suggests that AspH could potentially play a role in redox regulation and potentially hypoxia sensing.

PHD2 binds Fe(II) and 2OG in an unusually stable manner (74), leading to the proposal the PHDs have evolved to focus on hypoxia sensing (although PHD activity can likely be limited by

Fe(II) and, maybe, 2OG availability in some circumstances). Further work on AspH is required to determine the stability of its Fe(II)·2OG complex in the absence of substrate, although AspH does not catalyze 2OG oxidation efficiently in the absence of substrate (36). AspH is up-regulated in response to hypoxia at least in some cell lines (likely in a HIF-promoted manner) (75, 76, 77), potentially to compensate for reduction in AspH hydroxylase activity at lower O_2 concentrations. Some other human 2OG oxygenases are up-regulated by hypoxia (77), including the hypoxia sensors PHD2 (78, 79) and, especially, PHD3 (75, 80). A potential role for AspH in hypoxic regulation is thus consistent with its observed strong up-regulation in hypoxia in cells (75, 76, 77), including in hypoxic tumors (13, 15, 81). Further investigations should be directed to determine AspH substrate hydroxylation levels *in vivo* as a function of O_2 availability and disease. The results might help to decipher the mechanism of how AspH impacts on cell motility and the molecular function(s) of Asp/Asn hydroxylation.

In general, EGFDs manifest high sequence variability (82), which could explain differences in observed *in vivo* EGFD hydroxylation levels. This hypothesis is supported by the observation that, at least for the tested substrates, the AspH kinetic parameters for the stable thioether-linked cyclic peptides appear to reflect *in vivo* observed AspH substrate hydroxylation levels well (Tables 1 and 2). This observation means that thioether-linked cyclic peptides based on the sequences of AspH substrate EGFDs might be used to predict *in vivo* EGFD hydroxylation levels of AspH substrates that have not previously been validated *in vivo*. In this regard, the human EGFL7 protein, which is a target of HIF and is up-regulated in hypoxia (83) and which contains an EGFD bearing the AspH substrate consensus sequence, is one interesting example (84). EGFL7 is proposed to have roles in angiogenesis (85, 86) and the promotion of cell motility in human cancers (*e.g.* hepatocellular carcinoma (87), prostate cancer (88), and gastric cancer (89)). EGFL7 might thus constitute a disease-linked physiologically relevant AspH substrate (87–89). A cyclic peptide based on the sequence of EGFL7 is an efficient AspH substrate (Figs. 2 and 5*e*). Further cell-based experiments should be performed to investigate the biological relevance of this result.

EGFD disulfide isomerization may be of *in vivo* relevance with respect to AspH function (36). Indeed, the imperfect lack of correlation between the observed *in vitro* and *in vivo* AspH substrate hydroxylation levels may reflect complex regulatory factors, potentially involving context-dependent variations in disulfide patterns.

Several human 2OG oxygenases are being pursued as drug targets, with inhibitors of the PHDs being recently approved for the treatment of anemia in chronic kidney disease (90, 91). At least in part, the mode of action of the clinically used compound mildronate is proposed to involve inhibition of γ-butyrobetaine hydroxylase, thereby altering cellular metabolism (92). Although AspH is not yet a validated medicinal chemistry (anticancer) target, the efficient AspH activity assay together with the kinetic parameters of AspH reported here will be useful in designing an AspH inhibition assay to develop small molecule probes to investigate AspH function *in vivo*. The assay will also be useful in profiling clinically administered and clinical candidate 2OG oxygenase inhibitors, with a view to help enabling safe medicines. In this regard, it may be that the unusual active site chemistry of AspH can be exploited to obtain selectivity.

Experimental procedures

General information

All chemicals were obtained from commercial sources (Sigma–Aldrich) and used as received. Milli Q ultrapure (MQ-grade) water was used for buffers; LC-MS grade solvents were used for SPE-MS. Co-factor/co-substrate stock solutions (LAA: 50 mM in MQ-grade water; 2OG: 10 mM in MQ-grade water; ammonium iron(II) sulfate hexahydrate, FAS, $(NH_4)_2Fe(SO_4)_2{\cdot}6H_2O$: 400 mM in 20 mM HCl diluted to 1 mM in MQ-grade water) were freshly prepared from commercial solids each day AspH assays were performed.

Recombinant AspH production and purification

Reported procedures were used (36). In brief, a pET-28a(+) vector encoding for N-terminal His_6-tagged $AspH_{315–758}$ (His_6–$AspH_{315–758}$) was transformed into *Escherichia coli* BL21 (DE3) cells. The resultant cells were grown in 2TY medium supplemented with kanamycin (0.05 mM) at 37 °C with shaking (180 rpm). AspH production was induced at an A_{600} of ~1.2 at 18 °C by adding isopropyl β-D-thiogalactopyranoside (1 M) to a final concentration of 0.1 mM. The cells were shaken for 16 h at 18 °C and harvested by centrifugation (8000 rpm, 8 min, 4 °C); the resultant cell pellets were stored at −80 °C. Frozen cells were resuspended (30 g/100 ml) in ice-cold 50 mM HEPES buffer (pH 7.5, 500 mM NaCl, 5 mM imidazole) containing EDTA-free protease inhibitor mixture tablets (1 tablet/50 ml; Roche Diagnostics or Sigma–Aldrich) and DNase I (bovine pancreas, grade II; Roche Diagnostics). The cells were lysed by sonication on ice (eight 30-s bursts; Sonics Vibra-Cell VCX500, amplitude: 60%), and the lysates were then centrifuged (20,000 rpm, 30 min, 4 °C). The supernatant containing AspH was purified at 4 °C by Ni(II)-affinity chromatography (HisTrap HP column, GE Healthcare; 1 ml/min flow rate) using an ÄKTA Pure machine (GE Healthcare) with a gradient of wash (50 mM HEPES, pH 7.5, 500 mM NaCl, 40 mM imidazole) and elution buffers (50 mM HEPES, pH 7.5, 500 mM NaCl, 500 mM imidazole). Eluted fractions containing AspH were pooled, then concentrated using an Amicon Ultra centrifugal filter (4000 rpm, 4 °C), and further purified by size-exclusion chromatography using a HiLoad 26/60 Superdex 75 pg 300-ml column with a flow rate of 1 ml/min and 50 mM HEPES (pH 7.5, 150 mM NaCl) as elution buffer. AspH was >95% pure by SDS-PAGE analysis and had the anticipated mass as reported (36). His_6–$AspH_{315–758}$ was stored in 50 mM HEPES buffer (pH 7.5, 150 mM NaCl) at a concentration of 125 μM at −78 °C; fresh aliquots were used for all biochemical experiments.

AspH substrates

AspH substrates were initially designed based on the sequence of EGFD1 of human coagulation factor X (hFX amino acids 86–124) (6, 7); all were prepared with a C-terminal amide. The hFX–$EGFD1_{86–124}$ peptide (Fig. 1*b*, *peptide 1/2*) was synthesized by solid-phase peptide synthesis (SPPS) with the disul-

fide bridges being formed by thiol-oxidation in air-saturated buffer and purified by Peptide Synthetics (Peptide Protein Research Ltd, UK). The hFX–EGFD1$_{86-124}$-4Ser peptide (Fig. 1*b*, *peptide 3*) was synthesized by SPPS and purified by GL Biochem (Shanghai) Ltd (Shanghai, China).

The thioether-linked cyclic peptide hFX–CP$_{101-119}$ (hFX amino acids 101–119; Fig. 1*b*, *peptide 4*) was synthesized from the corresponding linear peptide (D-Ala replacing Cys101$_{hFX}$ and Ser replacing Cys112$_{hFX}$) which was obtained by SPPS using the Fmoc-protection strategy (36). Microwave-assisted SPPS was performed using an automated peptide synthesizer (Liberty Blue, CEM Corporation) from the C to N termini on Rink Amide MBHA resin (AGTC Bioproducts; loading: 0.6–0.8 mmol/g) using iterative coupling (90 °C; 140 s; *N*,*N*-diisopropylcarbodiimide, Oxyma, Hünig's base, Fmoc-protected amino acids) and deprotection steps (90 °C; 90 s; 80/20% (v/v) DMF/piperidine). The N-terminal amine of the linear peptide was capped on the resin using *N*-chloroacetylsuccinimide. The linear peptide was cleaved from the resin and deprotected using a mixture of TFA, triisopropylsilane, 1,3-dimethoxybenzene, and water (92.5/2.5/2.5/2.5% (v/v/v/v), respectively). The solids were separated, and the linear peptide was precipitated from the solution using cold diethyl ether. The solid linear peptide was dissolved in water/acetonitrile, lyophilized, dissolved in aqueous triethylammonium acetate buffer (1 M, pH 8.5)/acetonitrile, and cyclized in a microwave reactor (Biotage Initiator, 10 min at 80 °C) (93). The crude product was filtered and directly purified using a semipreparative HPLC machine (JASCO) equipped with a reverse-phase column (Gemini 00G-4454-U0-AX; phase NX-C18). A linear gradient (0–30% (v/v) over 35 min) of acetonitrile in deoxygenated MQ-grade water (each containing 0.1% (v/v) TFA) was used as eluent. Fractions containing the cyclic peptide hFX–CP$_{101-119}$ (t_R = 34.4 min) were combined, lyophilized, and analyzed by MS.

The thioether-linked cyclic peptides hFVII–CP$_{121-139}$, hFIX–CP$_{108-126}$, hProC–CP$_{111-129}$, hC1r–CP$_{165-183}$, hC1s–CP$_{147-165}$, hFXII–CP$_{110-128}$, and hEGFL7–CP$_{152-170}$ were designed based on the amino acid sequence of the EGFDs of the corresponding human proteins and prepared as described above. The details are given in Fig. S4.

AspH activity assays

The substrate mixture (1.0 ml) containing 2.4 μM peptide, 120 μM LAA, 12 μM FAS, and 12 μM 2OG in 50 mM HEPES buffer (pH 7.5) was added into a well of a 2-ml volume 96-well assay plate (Greiner) at 20 °C under an ambient atmosphere. A blank sample was analyzed using a RapidFire RF 360 high-throughput sampling robot (Agilent) attached to an Agilent 6530 accurate mass quadrupole TOF mass spectrometer operated in the positive ionization mode. The enzyme mixture (0.2 ml), containing 0.6 μM His$_6$–AspH$_{315-758}$ in 50 mM HEPES buffer (pH 7.5), was then added to the well and thoroughly mixed. The RapidFire sampling robot was programmed to analyze 1 sample/min. The following SPE-MS conditions were used: assay samples were aspirated under vacuum for 0.4 s and loaded onto a C4 SPE cartridge. After loading, the C4 SPE cartridge was washed with 0.1% (v/v) aqueous formic acid to remove nonvolatile buffer salts (5 s, 1.5 ml/min). The peptide was then eluted from the SPE cartridge with 0.1% (v/v) aqueous formic acid in 85/15 (v/v) acetonitrile/water into the mass spectrometer (5 s, 1.25 ml/min). The SPE cartridge was re-equilibrated with 0.1% (v/v) aqueous formic acid (1 s, 1.25 ml/min). The mass spectrometer parameters were capillary voltage (3500 V), fragmentor voltage (150 V), gas temperature (350 °C), gas flow (12 liters/min). The m/z + 2 charge states of the substrate peptide and the product (hydroxylated) peptide were used to extract ion chromatogram data; peak areas were integrated using RapidFire Integrator software (Agilent). The data were exported into Microsoft Excel and used to calculate the percentage of conversion of the hydroxylation reaction using the equation: % conversion = 100 × (integral product peptide)/(integral substrate peptide + integral product peptide).

Determination of kinetic parameters

Maximum velocities (v_{max} or v_{max}^{app} monitoring hFX–CP$_{101-119}$ turnover) and Michaelis constants (K_m or K_m^{app} monitoring hFX–CP$_{101-119}$ turnover) of AspH were determined in independent triplicates for LAA, Fe(II), 2OG, and cyclic peptide AspH substrates by SPE-MS. An enzyme mixture (0.1 ml) containing 0.6 μM His$_6$–AspH$_{315-758}$ in 50 mM HEPES buffer (pH 7.5) was added at 20 °C to a substrate mixture (0.5 ml) containing peptide substrate and co-factors (1.2× final concentration) in 50 mM HEPES buffer (pH 7.5). Final substrate and co-factor/co-substrate concentrations are given in Fig. S6. The reactions were monitored with a rate of 1 sample/25 s using the same SPE-MS configuration as described above. The data were analyzed as described above, and the slopes of the initial reaction rates (Fig. S6) were fitted to a Michaelis–Menten plot using nonlinear regression (GraphPad Prism 5).

For determining v_{max}^{app} and K_m^{app} of AspH for O_2, 2.2 μM hFX–CP$_{101-119}$ (65 μl) in 50 mM HEPES (pH 7.5) were exposed in a gas-tight glass vial to variable O_2 concentrations (in nitrogen; Fig. S7) using a mass flow controller (32). After equilibrating the atmosphere, co-factor and co-substrates were added by syringe (1.5 μl of 4.7 mM LAA and 0.99 mM 2OG in MQ-grade water and 1.5 μl of 0.99 mM FAS in MQ-grade water) followed by 2.0 μl of 3.5 μM His$_6$–AspH$_{315-758}$ in 50 mM HEPES (pH 7.5) at 20 °C. The enzyme reaction was stopped after the indicated reaction time by the addition of 15% (v/v) aqueous formic acid (4 μl) and analyzed by SPE-MS using the configurations given above; the experiments were performed in independent quadruplicates. The data were analyzed as described, and the slopes of the initial reaction rates (Fig. S7) were fitted to a Michaelis–Menten plot using nonlinear regression (GraphPad Prism 5).

To determine turnover numbers (k_{cat}), the AspH active sites were titrated in independent triplicates using pyridine-2,4-dicarboxylic acid as a tight binding AspH inhibitor (38, 54). Final inhibitor concentrations (in DMSO) are given in Fig. S5. The enzyme mixture (0.1 ml), containing 0.6 μM His$_6$–AspH$_{315-758}$ in 50 mM HEPES buffer (pH 7.5), was incubated with 1% (v/v) DMSO inhibitor solution for 15 min at 20 °C. This was then added to the substrate mixture (0.5 ml), containing 2.4 μM hFX–CP$_{101-119}$, 120 μM LAA, 2.4 μM FAS, 3.6 μM 2OG, and 1% (v/v) DMSO inhibitor solution in 50 mM HEPES buffer (pH 7.5). The reactions were monitored by SPE-MS with a rate of 1 sample/25 s using identical configurations as before. The data were

analyzed as described, and the slopes of the initial reaction rates (Fig. S5) were fitted to a Morrison plot using nonlinear regression (GraphPad Prism 5) with the following constraints: 0 < enzyme active sites ($[E]_T$) < 0.1 μM; K_m^{app} (2OG) = 0.6 μM; concentration (2OG) = 3.0 μM. The Morrison equation is as follows, where I is the inhibitor concentration, K_i is the dissociation constant of the inhibitor, E_T is the total concentration of active enzyme, and v_i/v_0 is the fractional enzyme activity (94).

$$\frac{v_i}{v_0} = \left(1 - \frac{[E]_T + [I] + (K_i \cdot (1 + [S]/K_{m,app}) - \sqrt{([E]_T + [I] + K_i \cdot (1 + [S]/K_{m,app}))^2 - 4[E]_T[I]}}{2[E]_T}\right) \quad \text{(Eq. 1)}$$

Author contributions—L. B. and A. T. data curation; L. B. and A. T. formal analysis; L. B. and C. J. S. funding acquisition; L. B., A. T., and C. J. S. validation; L. B. and A. T. investigation; L. B. and A. T. visualization; L. B. and A. T. methodology; L. B. and C. J. S. writing-original draft; L. B., A. T., and C. J. S. writing-review and editing; C. J. S. conceptualization; C. J. S. supervision.

References

1. Stenflo, J., Holme, E., Lindstedt, S., Chandramouli, N., Huang, L. H., Tam, J. P., and Merrifield, R. B. (1989) Hydroxylation of aspartic acid in domains homologous to the epidermal growth factor precursor is catalyzed by a 2-oxoglutarate-dependent dioxygenase. *Proc. Natl. Acad. Sci. U.S.A.* **86,** 444–447 CrossRef Medline
2. Korioth, F., Gieffers, C., and Frey, J. (1994) Cloning and characterization of the human gene encoding aspartyl β-hydroxylase. *Gene* **150,** 395–399 CrossRef Medline
3. Stenflo, J. (1991) Structure-function relationships of epidermal growth factor modules in vitamin K–dependent clotting factors. *Blood* **78,** 1637–1651 CrossRef Medline
4. Hynes, R. O. (2009) The extracellular matrix: not just pretty fibrils. *Science* **326,** 1216–1219 CrossRef Medline
5. Kanzaki, T., Olofsson, A., Morén, A., Wernstedt, C., Hellman, U., Miyazono, K., Claesson-Welsh, L., and Heldin, C.-H. (1990) TGF-β1 binding protein: a component of the large latent complex of TGF-β1 with multiple repeat sequences. *Cell* **61,** 1051–1061 CrossRef Medline
6. McMullen, B. A., Fujikawa, K., Kisiel, W., Sasagawa, T., Howald, W. N., Kwa, E. Y., and Weinstein, B. (1983) Complete amino acid sequence of the light chain of human blood coagulation factor X: evidence for identification of residue 63 as β-hydroxyaspartic acid. *Biochemistry* **22,** 2875–2884 CrossRef Medline
7. Fernlund, P., and Stenflo, J. (1983) β-Hydroxyaspartic acid in vitamin K–dependent proteins. *J. Biol. Chem.* **258,** 12509–12512 Medline
8. Thim, L., Bjoern, S., Christensen, M., Nicolaisen, E. M., Lund-Hansen, T., Pedersen, A. H., and Hedner, U. (1988) Amino acid sequence and post-translational modifications of human factor VIIa from plasma and transfected baby hamster kidney cells. *Biochemistry* **27,** 7785–7793 CrossRef Medline
9. Patel, N., Khan, A. O., Mansour, A., Mohamed, J. Y., Al-Assiri, A., Haddad, R., Jia, X., Xiong, Y., Mégarbané, A., Traboulsi, E. I., and Alkuraya, F. S. (2014) Mutations in ASPH cause facial dysmorphism, lens dislocation, anterior-segment abnormalities, and spontaneous filtering blebs, or Traboulsi syndrome. *Am. J. Hum. Genet.* **94,** 755–759 CrossRef Medline
10. Abarca Barriga, H. H., Caballero, N., Trubnykova, M., Castro-Mujica, M. D. C., La Serna-Infantes, J. E., Vásquez, F., and Hennekam, R. C. (2018) A novel ASPH variant extends the phenotype of Shawaf–Traboulsi syndrome. *Am. J. Med. Genet. A* **176,** 2494–2500 CrossRef Medline
11. Siggs, O. M., Souzeau, E., and Craig, J. E. (2019) Loss of ciliary zonule protein hydroxylation and lens stability as a predicted consequence of biallelic ASPH variation. *Ophthalmic Genet.* **40,** 12–16 CrossRef Medline
12. Dinchuk, J. E., Focht, R. J., Kelley, J. A., Henderson, N. L., Zolotarjova, N. I., Wynn, R., Neff, N. T., Link, J., Huber, R. M., Burn, T. C., Rupar, M. J., Cunningham, M. R., Selling, B. H., Ma, J., Stern, A. A., *et al.* (2002) Absence of post-translational aspartyl β-hydroxylation of epidermal growth factor domains in mice leads to developmental defects and an increased incidence of intestinal neoplasia. *J. Biol. Chem.* **277,** 12970–12977 CrossRef Medline
13. Lavaissiere, L., Jia, S., Nishiyama, M., de la Monte, S., Stern, A. M., Wands, J. R., and Friedman, P. A. (1996) Overexpression of human aspartyl(asparaginyl)β-hydroxylase in hepatocellular carcinoma and cholangiocarcinoma. *J. Clin. Invest.* **98,** 1313–1323 CrossRef Medline
14. Sturla, L.-M., Tong, M., Hebda, N., Gao, J., Thomas, J.-M., Olsen, M., and de la Monte, S. M. (2016) Aspartate-β-hydroxylase (ASPH): a potential therapeutic target in human malignant gliomas. *Heliyon* **2,** e00203 CrossRef Medline
15. Ince, N., de la Monte, S. M., and Wands, J. R. (2000) Overexpression of human aspartyl (asparaginyl) β-hydroxylase is associated with malignant transformation. *Cancer Res.* **60,** 1261–1266 Medline
16. Zou, Q., Hou, Y., Wang, H., Wang, K., Xing, X., Xia, Y., Wan, X., Li, J., Jiao, B., Liu, J., Huang, A., Wu, D., Xiang, H., Pawlik, T. M., Wang, H., *et al.* (2018) Hydroxylase activity of ASPH promotes hepatocellular carcinoma metastasis through epithelial-to-mesenchymal transition pathway. *EBioMedicine* **31,** 287–298 CrossRef Medline
17. Yang, H., Song, K., Xue, T., Xue, X. P., Huyan, T., Wang, W., and Wang, H. (2010) The distribution and expression profiles of human aspartyl/asparaginyl β-hydroxylase in tumor cell lines and human tissues. *Oncol. Rep.* **24,** 1257–1264 Medline
18. de la Monte, S. M., Tamaki, S., Cantarini, M. C., Ince, N., Wiedmann, M., Carter, J. J., Lahousse, S. A., Califano, S., Maeda, T., Ueno, T., D'Errico, A., Trevisani, F., and Wands, J. R. (2006) Aspartyl-(asparaginyl)-β-hydroxylase regulates hepatocellular carcinoma invasiveness. *J. Hepatol.* **44,** 971–983 CrossRef Medline
19. Lawton, M., Tong, M., Gundogan, F., Wands, J. R., and de la Monte, S. M. (2010) Aspartyl-(asparaginyl) β-hydroxylase, hypoxia-inducible factor-1α and notch cross-talk in regulating neuronal motility. *Oxid. Med. Cell Longev.* **3,** 347–356 CrossRef Medline
20. Aihara, A., Huang, C.-K., Olsen, M. J., Lin, Q., Chung, W., Tang, Q., Dong, X., and Wands, J. R. (2014) A cell-surface β-hydroxylase is a biomarker and therapeutic target for hepatocellular carcinoma. *Hepatology* **60,** 1302–1313 CrossRef Medline
21. Huang, C.-K., Iwagami, Y., Aihara, A., Chung, W., de la Monte, S., Thomas, J.-M., Olsen, M., Carlson, R., Yu, T., Dong, X., and Wands, J. (2016) Anti-tumor effects of second generation β-hydroxylase inhibitors on cholangiocarcinoma development and progression. *PLoS One* **11,** e0150336 CrossRef Medline
22. Chillakuri, C. R., Sheppard, D., Lea, S. M., and Handford, P. A. (2012) Notch receptor–ligand binding and activation: insights from molecular studies. *Semin. Cell Dev. Biol.* **23,** 421–428 CrossRef Medline
23. Kaelin, W. G., Jr., and Ratcliffe, P. J. (2008) Oxygen sensing by metazoans: the central role of the HIF hydroxylase pathway. *Mol. Cell* **30,** 393–402 CrossRef Medline
24. Schofield, C. J., and Ratcliffe, P. J. (2004) Oxygen sensing by HIF hydroxylases. *Nat. Rev. Mol. Cell Biol.* **5,** 343–354 CrossRef Medline
25. (2015) *2-Oxoglutarate-dependent Oxygenases* (Schofield, C. J., and Hausinger, R. P., eds) Royal Society of Chemistry, Cambridge, UK
26. Hirsilä, M., Koivunen, P., Günzler, V., Kivirikko, K. I., and Myllyharju, J. (2003) Characterization of the human prolyl 4-hydroxylases that modify the hypoxia-inducible factor. *J. Biol. Chem.* **278,** 30772–30780 CrossRef Medline
27. Ehrismann, D., Flashman, E., Genn, D. N., Mathioudakis, N., Hewitson, K. S., Ratcliffe, P. J., and Schofield, C. J. (2007) Studies on the activity of the hypoxia-inducible-factor hydroxylases using an oxygen consumption assay. *Biochem. J.* **401,** 227–234 CrossRef Medline
28. Dao, J. H., Kurzeja, R. J., Morachis, J. M., Veith, H., Lewis, J., Yu, V., Tegley, C. M., and Tagari, P. (2009) Kinetic characterization and identification of a novel inhibitor of hypoxia-inducible factor prolyl hydroxylase 2 using a time-resolved fluorescence resonance energy transfer-based assay technology. *Anal. Biochem.* **384,** 213–223 CrossRef Medline
29. Flashman, E., Hoffart, L. M., Hamed, R. B., Bollinger, J. M., Jr., Krebs, C., and Schofield, C. J. (2010) Evidence for the slow reaction of hypoxia-

inducible factor prolyl hydroxylase 2 with oxygen. *FEBS J.* **277,** 4089–4099 CrossRef Medline

30. Koivunen, P., Hirsilä, M., Günzler, V., Kivirikko, K. I., and Myllyharju, J. (2004) Catalytic properties of the asparaginyl hydroxylase (FIH) in the oxygen sensing pathway are distinct from those of its prolyl 4-hydroxylases. *J. Biol. Chem.* **279,** 9899–9904 CrossRef Medline
31. Wilkins, S. E., Hyvärinen, J., Chicher, J., Gorman, J. J., Peet, D. J., Bilton, R. L., and Koivunen, P. (2009) Differences in hydroxylation and binding of notch and HIF-1α demonstrate substrate selectivity for factor inhibiting HIF-1 (FIH-1). *Int. J. Biochem. Cell Biol.* **41,** 1563–1571 CrossRef Medline
32. Tarhonskaya, H., Hardy, A. P., Howe, E. A., Loik, N. D., Kramer, H. B., McCullagh, J. S., Schofield, C. J., and Flashman, E. (2015) Kinetic investigations of the role of factor inhibiting hypoxia-inducible factor (FIH) as an oxygen sensor. *J. Biol. Chem.* **290,** 19726–19742 CrossRef Medline
33. Cockman, M. E., Lancaster, D. E., Stolze, I. P., Hewitson, K. S., McDonough, M. A., Coleman, M. L., Coles, C. H., Yu, X., Hay, R. T., Ley, S. C., Pugh, C. W., Oldham, N. J., Masson, N., Schofield, C. J., and Ratcliffe, P. J. (2006) Posttranslational hydroxylation of ankyrin repeats in IκB proteins by the hypoxia-inducible factor (HIF) asparaginyl hydroxylase, factor inhibiting HIF (FIH). *Proc. Natl. Acad. Sci. U.S.A.* **103,** 14767–14772 CrossRef Medline
34. Coleman, M. L., McDonough, M. A., Hewitson, K. S., Coles, C., Mecinovic, J., Edelmann, M., Cook, K. M., Cockman, M. E., Lancaster, D. E., Kessler, B. M., Oldham, N. J., Ratcliffe, P. J., and Schofield, C. J. (2007) Asparaginyl hydroxylation of the notch ankyrin repeat domain by factor inhibiting hypoxia-inducible factor. *J. Biol. Chem.* **282,** 24027–24038 CrossRef Medline
35. Yang, M., Ge, W., Chowdhury, R., Claridge, T. D., Kramer, H. B., Schmierer, B., McDonough, M. A., Gong, L., Kessler, B. M., Ratcliffe, P. J., Coleman, M. L., and Schofield, C. J. (2011) Asparagine and aspartate hydroxylation of the cytoskeletal ankyrin family is catalyzed by factor-inhibiting hypoxia–inducible factor. *J. Biol. Chem.* **286,** 7648–7660 CrossRef Medline
36. Pfeffer, I., Brewitz, L., Krojer, T., Jensen, S. A., Kochan, G. T., Kershaw, N. J., Hewitson, K. S., McNeill, L. A., Kramer, H., Münzel, M., Hopkinson, R. J., Oppermann, U., Handford, P. A., McDonough, M. A., and Schofield, C. J. (2019) Aspartate/asparagine–β-hydroxylase crystal structures reveal an unexpected epidermal growth factor–like domain substrate disulfide pattern. *Nat. Commun.* **10,** 4910 CrossRef Medline
37. Gronke, R. S., VanDusen, W. J., Garsky, V. M., Jacobs, J. W., Sardana, M. K., Stern, A. M., and Friedman, P. A. (1989) Aspartyl β-hydroxylase: *in vitro* hydroxylation of a synthetic peptide based on the structure of the first growth factor-like domain of human factor IX. *Proc. Natl. Acad. Sci. U.S.A.* **86,** 3609–3613 CrossRef Medline
38. Gronke, R. S., Welsch, D. J., VanDusen, W. J., Garsky, V. M., Sardana, M. K., Stern, A. M., and Friedman, P. A. (1990) Partial purification and characterization of bovine liver aspartyl β-hydroxylase. *J. Biol. Chem.* **265,** 8558–8565 Medline
39. Wang, Q. P., VanDusen, W. J., Petroski, C. J., Garsky, V. M., Stern, A. M., and Friedman, P. A. (1991) Bovine liver aspartyl β-hydroxylase. Purification and characterization. *J. Biol. Chem.* **266,** 14004–14010 Medline
40. McGinnis, K., Ku, G. M., VanDusen, W. J., Fu, J., Garsky, V., Stern, A. M., and Friedman, P. A. (1996) Site-directed mutagenesis of residues in a conserved region of bovine aspartyl (asparaginyl) β-hydroxylase: evidence that histidine 675 has a role in binding Fe^{2+}. *Biochemistry* **35,** 3957–3962 CrossRef Medline
41. Hutchinson, S. E., Leveridge, M. V., Heathcote, M. L., Francis, P., Williams, L., Gee, M., Munoz-Muriedas, J., Leavens, B., Shillings, A., Jones, E., Homes, P., Baddeley, S., Chung C.-W., Bridges, A., and Argyrou, A. (2012) Enabling lead discovery for histone lysine demethylases by high-throughput RapidFire mass spectrometry. *J. Biomol. Screen.* **17,** 39–48 CrossRef Medline
42. Mulji, A., Haslam, C., Brown, F., Randle, R., Karamshi, B., Smith, J., Eagle, R., Munoz-Muriedas, J., Taylor, J., Sheikh, A., Bridges, A., Gill, K., Jepras, R., Smee, P., Barker, M., *et al.* (2012) Configuration of a high-content imaging platform for hit identification and pharmacological assessment of JMJD3 demethylase enzyme inhibitors. *J. Biomol. Screen.* **17,** 108–120 CrossRef Medline
43. Gerken, P. A., Wolstenhulme, J. R., Tumber, A., Hatch, S. B., Zhang, Y., Müller, S., Chandler, S. A., Mair, B., Li, F., Nijman, S. M. B., Konietzny, R., Szommer, T., Yapp, C., Fedorov, O., Benesch, J. L. P., *et al.* (2017) Discovery of a highly selective cell-active inhibitor of the histone lysine demethylases KDM2/7. *Angew. Chem. Int. Ed. Engl.* **56,** 15555–15559 CrossRef Medline
44. Westaway, S. M., Preston, A. G., Barker, M. D., Brown, F., Brown, J. A., Campbell, M., Chung, C.-W., Diallo, H., Douault, C., Drewes, G., Eagle, R., Gordon, L., Haslam, C., Hayhow, T. G., Humphreys, P. G., *et al.* (2016) Cell penetrant inhibitors of the KDM4 and KDM5 families of histone lysine demethylases: 1. 3-Amino-4-pyridine carboxylate derivatives. *J. Med. Chem.* **59,** 1357–1369 CrossRef Medline
45. Holt-Martyn, J. P., Tumber, A., Rahman, M. Z., Lippl, K., Figg, W., Jr., McDonough, M. A., Chowdhury, R., and Schofield, C. J. (2019) Studies on spiro[4.5]decanone prolyl hydroxylase domain inhibitors. *MedChemComm* **10,** 500–504 CrossRef Medline
46. Myllylä, R., Majamaa, K., Günzler, V., Hanauske-Abel, H. M., and Kivirikko, K. I. (1984) Ascorbate is consumed stoichiometrically in the uncoupled reactions catalyzed by prolyl 4-hydroxylase and lysyl hydroxylase. *J. Biol. Chem.* **259,** 5403–5405 Medline
47. Flashman, E., Davies, S. L., Yeoh, K. K., and Schofield, C. J. (2010) Investigating the dependence of the hypoxia-inducible factor hydroxylases (factor inhibiting HIF and prolyl hydroxylase domain 2) on ascorbate and other reducing agents. *Biochem. J.* **427,** 135–142 CrossRef Medline
48. Osipyants, A. I., Poloznikov, A. A., Smirnova, N. A., Hushpulian, D. M., Khristichenko, A. Y., Chubar, T. A., Zakhariants, A. A., Ahuja, M., Gaisina, I. N., Thomas, B., Brown, A. M., Gazaryan, I. G., and Tishkov, V. I. (2018) L- ascorbic acid: a true substrate for HIF prolyl hydroxylase? *Biochimie* **147,** 46–54 CrossRef Medline
49. Drakenberg, T., Fernlund, P., Roepstorff, P., and Stenflo, J. (1983) β-Hydroxyaspartic acid in vitamin K–dependent protein C. *Proc. Natl. Acad. Sci. U.S.A.* **80,** 1802–1806 CrossRef Medline
50. Harris, R. J., Ling, V. T., and Spellman, M. W. (1992) *O*-Linked fucose is present in thes first epidermal growth factor domain of factor XII but not protein C. *J. Biol. Chem.* **267,** 5102–5107 Medline
51. Przysiecki, C. T., Staggers, J. E., Ramjit, H. G., Musson, D. G., Stern, A. M., Bennett, C. D., and Friedman, P. A. (1987) Occurrence of β-hydroxylated asparagine residues in non–vitamin K–dependent proteins containing epidermal growth factor–like domains. *Proc. Natl. Acad. Sci. U.S.A.* **84,** 7856–7860 CrossRef Medline
52. Arlaud, G. J., Van Dorsselaer, A., Bell, A., Mancini, M., Aude, C., and Gagnon, J. (1987) Identification of erythro-β-hydroxyasparagine in the EGF-like domain of human C1r. *FEBS Lett.* **222,** 129–134 CrossRef Medline
53. Thielens, N. M., Van Dorsselaer, A., Gagnon, J., and Arlaud, G. J. (1990) Chemical and functional characterization of a fragment of C1s containing the epidermal growth factor homology region. *Biochemistry* **29,** 3570–3578 CrossRef Medline
54. Derian, C. K., VanDusen, W., Przysiecki, C. T., Walsh, P. N., Berkner, K. L., Kaufman, R. J., and Friedman, P. A. (1989) Inhibitors of 2-ketoglutarate-dependent dioxygenases block aspartyl β-hydroxylation of recombinant human factor IX in several mammalian expression systems. *J. Biol. Chem.* **264,** 6615–6618 Medline
55. Xue, J.-H., Chen, G.-D., Hao, F., Chen, H., Fang, Z., Chen, F.-F., Pang, B., Yang, Q.-L., Wei, X., Fan, Q.-Q., Xin, C., Zhao, J., Deng, X., Wang, B.-A., Zhang, X.-J., *et al.* (2019) A vitamin-C-derived DNA modification catalysed by an algal TET homologue. *Nature* **569,** 581–585 CrossRef Medline
56. Seo, Y. S., Yoo, A., Jung, J., Sung, S.-K., Yang, D. R., Kim, W. T., and Lee, W. (2004) The active site and substrate-binding mode of 1-aminocyclopropane-1-carboxylate oxidase determined by site-directed mutagenesis and comparative modelling studies. *Biochem. J.* **380,** 339–346 CrossRef Medline
57. Dilley, D. R., Wang, Z., Kadirjan-Kalbach, D. K., Ververidis, F., Beaudry, R., and Padmanabhan, K. (2013) 1-Aminocyclopropane-1-carboxylic acid oxidase reaction mechanism and putative post-translational activities of the ACCO protein. *AoB Plants* **5,** plt031 Medline
58. Grady, J. K., Chasteen, N. D., and Harris, D. C. (1988) Radicals from "Good's" buffers. *Anal. Biochem.* **173,** 111–115 CrossRef Medline
59. Chen, Q., Espey, M. G., Krishna, M. C., Mitchell, J. B., Corpe, C. P., Buettner, G. R., Shacter, E., and Levine, M. (2005) Pharmacologic ascorbic acid concentrations selectively kill cancer cells: action as a pro-drug to deliver hydrogen peroxide to tissues. *Proc. Natl. Acad. Sci. U.S.A.* **102,** 13604–13609 CrossRef Medline

60. Koivunen, P., Hirsilä, M., Remes, A. M., Hassinen, I. E., Kivirikko, K. I., and Myllyharju, J. (2007) Inhibition of hypoxia-inducible factor (HIF) hydroxylases by citric acid cycle intermediates: possible links between cell metabolism and stabilization of HIF. *J. Biol. Chem.* **282,** 4524–4532 CrossRef Medline
61. Huergo, L. F., and Dixon, R. (2015) The emergence of 2-oxoglutarate as a master regulator metabolite. *Microbiol. Mol. Biol. Rev.* **79,** 419–435 CrossRef Medline
62. Rydzik, A. M., Leung, I. K., Kochan, G. T., Thalhammer, A., Oppermann, U., Claridge, T. D., and Schofield, C. J. (2012) Development and application of a fluoride-detection-based fluorescence assay for γ-butyrobetaine hydroxylase. *ChemBioChem* **13,** 1559–1563 CrossRef Medline
63. Chevreux, G., Tilly, N., Faid, V., and Bihoreau, N. (2015) Mass spectrometry based analysis of human plasma-derived factor X revealed novel post-translational modifications. *Protein Sci.* **24,** 1640–1648 CrossRef Medline
64. Cascella, B., and Mirica, L. M. (2012) Kinetic analysis of iron-dependent histone demethylases: α-ketoglutarate substrate inhibition and potential relevance to the regulation of histone demethylation in cancer cells. *Biochemistry* **51,** 8699–8701 CrossRef Medline
65. Chakraborty, A. A., Laukka, T., Myllykoski, M., Ringel, A. E., Booker, M. A., Tolstorukov, M. Y., Meng, Y. J., Meier, S. R., Jennings, R. B., Creech, A. L., Herbert, Z. T., McBrayer, S. K., Olenchock, B. A., Jaffe, J. D., Haigis, M. C., *et al.* (2019) Histone demethylase KDM6A directly senses oxygen to control chromatin and cell fate. *Science* **363,** 1217–1222 CrossRef Medline
66. Hancock, R. L., Masson, N., Dunne, K., Flashman, E., and Kawamura, A. (2017) The activity of JmjC histone lysine demethylase KDM4A is highly sensitive to oxygen concentrations. *ACS Chem. Biol.* **12,** 1011–1019 CrossRef Medline
67. Glanville, R. W., Qian, R. Q., McClure, D. W., and Maslen, C. L. (1994) Calcium binding, hydroxylation, and glycosylation of the precursor epidermal growth factor–like domains of fibrillin-1, the Marfan gene protein. *J. Biol. Chem.* **269,** 26630–26634 Medline
68. Rose, N. R., McDonough, M. A., King, O. N., Kawamura, A., and Schofield, C. J. (2011) Inhibition of 2-oxoglutarate dependent oxygenases. *Chem. Soc. Rev.* **40,** 4364–4397 CrossRef Medline
69. Koivunen, P., Hirsilä, M., Kivirikko, K. I., and Myllyharju, J. (2006) The length of peptide substrates has a marked effect on hydroxylation by the hypoxia-inducible factor prolyl 4-hydroxylases. *J. Biol. Chem.* **281,** 28712–28720 CrossRef Medline
70. Yang, M., Hardy, A. P., Chowdhury, R., Loik, N. D., Scotti, J. S., McCullagh, J. S., Claridge, T. D., McDonough, M. A., Ge, W., and Schofield, C. J. (2013) Substrate selectivity analyses of factor inhibiting hypoxia-inducible factor. *Angew. Chem. Int. Ed. Engl.* **52,** 1700–1704 CrossRef Medline
71. Horton, J. R., Upadhyay, A. K., Qi, H. H., Zhang, X., Shi, Y., and Cheng, X. (2010) Enzymatic and structural insights for substrate specificity of a family of jumonji histone lysine demethylases. *Nat. Struct. Mol. Biol.* **17,** 38–43 CrossRef Medline
72. Takeda, K., Ho, V. C., Takeda, H., Duan, L.-J., Nagy, A., and Fong, G.-H. (2006) Placental but not heart defects are associated with elevated hypoxia-inducible factor α levels in mice lacking prolyl hydroxylase domain protein 2. *Mol. Cell Biol.* **26,** 8336–8346 CrossRef Medline
73. Chowdhury, R., McDonough, M. A., Mecinović, J., Loenarz, C., Flashman, E., Hewitson, K. S., Domene, C., and Schofield, C. J. (2009) Structural basis for binding of hypoxia-inducible factor to the oxygen-sensing prolyl hydroxylases. *Structure* **17,** 981–989 CrossRef Medline
74. McNeill, L. A., Flashman, E., Buck, M. R., Hewitson, K. S., Clifton, I. J., Jeschke, G., Claridge, T. D., Ehrismann, D., Oldham, N. J., and Schofield, C. J. (2005) Hypoxia-inducible factor prolyl hydroxylase 2 has a high affinity for ferrous iron and 2-oxoglutarate. *Mol. BioSyst.* **1,** 321–324 CrossRef Medline
75. Elvidge, G. P., Glenny, L., Appelhoff, R. J., Ratcliffe, P. J., Ragoussis, J., and Gleadle, J. M. (2006) Concordant regulation of gene expression by hypoxia and 2-oxoglutarate-dependent dioxygenase inhibition: the role of HIF-1α, HIF-2α, and other pathways. *J. Biol. Chem.* **281,** 15215–15226 CrossRef Medline
76. Benita, Y., Kikuchi, H., Smith, A. D., Zhang, M. Q., Chung, D. C., and Xavier, R. J. (2009) An integrative genomics approach identifies hypoxia inducible factor-1 (HIF-1)-target genes that form the core response to hypoxia. *Nucleic Acids Res.* **37,** 4587–4602 CrossRef Medline
77. Pollard, P. J., Loenarz, C., Mole, D. R., McDonough, M. A., Gleadle, J. M., Schofield, C. J., and Ratcliffe, P. J. (2008) Regulation of jumonji-domain-containing histone demethylases by hypoxia-inducible factor (HIF)-1α. *Biochem. J.* **416,** 387–394 CrossRef Medline
78. Epstein, A. C., Gleadle, J. M., McNeill, L. A., Hewitson, K. S., O'Rourke, J., Mole, D. R., Mukherji, M., Metzen, E., Wilson, M. I., Dhanda, A., Tian, Y.-M., Masson, N., Hamilton, D. L., Jaakkola, P., Barstead, R., *et al.* (2001) *C. elegans* EGL-9 and mammalian homologs define a family of dioxygenases that regulate HIF by prolyl hydroxylation. *Cell* **107,** 43–54 CrossRef Medline
79. Metzen, E., Berchner-Pfannschmidt, U., Stengel, P., Marxsen, J. H., Stolze, I., Klinger, M., Huang, W. Q., Wotzlaw, C., Hellwig-Bürgel, T., Jelkmann, W., Acker, H., and Fandrey, J. (2003) Intracellular localisation of human HIF-1α hydroxylases: implications for oxygen sensing. *J. Cell Sci.* **116,** 1319–1326 CrossRef Medline
80. Pescador, N., Cuevas, Y., Naranjo, S., Alcaide, M., Villar, D., Landázuri, M. O., and del Peso, L. (2005) Identification of a functional hypoxia-responsive element that regulates the expression of the *egl* nine homologue 3 (*egln3*/*phd3*) gene. *Biochem. J.* **390,** 189–197 CrossRef Medline
81. McKeown, S. R. (2014) Defining normoxia, physoxia and hypoxia in tumours: implications for treatment response. *Br. J. Radiol.* **87,** 20130676 CrossRef Medline
82. Campbell, I. D., and Bork, P. (1993) Epidermal growth factor–like modules. *Curr. Opin. Struct. Biol.* **3,** 385–392 CrossRef
83. Liu, Y.-S., Huang, Z.-W., Qin, A.-Q., Huang, Y., Giordano, F., Lu, Q.-H., and Jiang, W.-D. (2015) The expression of epidermal growth factor–like domain 7 regulated by oxygen tension via hypoxia inducible factor (HIF)-1α activity. *Postgrad. Med.* **127,** 144–149 CrossRef Medline
84. Fitch, M. J., Campagnolo, L., Kuhnert, F., and Stuhlmann, H. (2004) Egfl7, a novel epidermal growth factor-domain gene expressed in endothelial cells. *Dev. Dyn.* **230,** 316–324 CrossRef Medline
85. Parker, L. H., Schmidt, M., Jin, S.-W., Gray, A. M., Beis, D., Pham, T., Frantz, G., Palmieri, S., Hillan, K., Stainier, D. Y., De Sauvage, F. J., and Ye, W. (2004) The endothelial-cell-derived secreted factor Egfl7 regulates vascular tube formation. *Nature* **428,** 754–758 CrossRef Medline
86. Nichol, D., Shawber, C., Fitch, M. J., Bambino, K., Sharma, A., Kitajewski, J., and Stuhlmann, H. (2010) Impaired angiogenesis and altered notch signaling in mice overexpressing endothelial Egfl7. *Blood* **116,** 6133–6143 CrossRef Medline
87. Wu, F., Yang, L.-Y., Li, Y.-F., Ou, D.-P., Chen, D.-P., and Fan, C. (2009) Novel role for epidermal growth factor–like domain 7 in metastasis of human hepatocellular carcinoma. *Hepatology* **50,** 1839–1850 CrossRef Medline
88. Ma, L., Jiang, K., Jiang, P., Chen, K., Shao, J., Yu, Z., and Deng, G. (2017) EGF like domain multiple 7 regulates the migration and invasion of prostate cancer cells. *Int. J. Clin. Exp. Pathol.* **10,** 5359–5365
89. Luo, B.-H., Xiong, F., Wang, J.-P., Li, J.-H., Zhong, M., Liu, Q.-L., Luo, G.-Q., Yang, X.-J., Xiao, N., Xie, B., Xiao, H., Liu, R.-J., Dong, C.-S., Wang, K.-S., and Wen, J.-F. (2014) Epidermal growth factor–like domain-containing protein 7 (EGFL7) enhances EGF receptor-AKT signaling, epithelial-mesenchymal transition, and metastasis of gastric cancer cells. *PLoS One* **9,** e99922 CrossRef Medline
90. Koury, M. J., and Haase, V. H. (2015) Anaemia in kidney disease: harnessing hypoxia responses for therapy. *Nat. Rev. Nephrol.* **11,** 394–410 CrossRef Medline
91. Rabinowitz, M. H. (2013) Inhibition of hypoxia-inducible factor prolyl hydroxylase domain oxygen sensors: tricking the body into mounting orchestrated survival and repair responses. *J. Med. Chem.* **56,** 9369–9402 CrossRef Medline
92. Sjakste, N., Gutcaits, A., and Kalvinsh, I. (2005) Mildronate: an antiischemic drug for neurological indications. *CNS Drug Rev.* **11,** 151–168 Medline
93. Kawamura, A., Münzel, M., Kojima, T., Yapp, C., Bhushan, B., Goto, Y., Tumber, A., Katoh, T., King, O. N., Passioura, T., Walport, L. J., Hatch, S. B., Madden, S., Müller, S., Brennan, P. E., *et al.* (2017) Highly selective inhibition of histone demethylases by de novo macrocyclic peptides. *Nat. Commun.* **8,** 14773 CrossRef Medline
94. Copeland, R. A. (2000) *Enzymes: A Practical Introduction to Structure, Mechanism, and Data Analysis*, Wiley-VCH, Weinheim, Germany